

RESEARCH ARTICLE

Open Access



Fever-like temperature impacts on *Staphylococcus aureus* and *Pseudomonas aeruginosa* interaction, physiology, and virulence both in vitro and in vivo

E. C. Solar Venero^{1,8}, M. B. Galeano^{1†}, A. Luqman^{2†}, M. M. Ricardi^{3†}, F. Serral^{4†}, D. Fernandez Do Porto⁴, S. A. Robaldi⁵, B. A. Z. Ashari², T. H. Muni², D. E. Egoburo⁵, S. Nemirovsky¹, J. Escalante⁶, B. Nishimura⁶, M. S. Ramirez⁶, F. Götz⁷ and P. M. Tribelli^{1,5*} 

Abstract

Background *Staphylococcus aureus* (SA) and *Pseudomonas aeruginosa* (PA) cause a wide variety of bacterial infections and coinfections, showing a complex interaction that involves the production of different metabolites and metabolic changes. Temperature is a key factor for bacterial survival and virulence and within the host, bacteria could be exposed to an increment in temperature during fever development. We analyzed the previously unexplored effect of fever-like temperatures (39 °C) on *S. aureus* USA300 and *P. aeruginosa* PAO1 microaerobic mono- and co-cultures compared with 37 °C, by using RNAseq and physiological assays including in vivo experiments.

Results In general terms both temperature and co-culturing had a strong impact on both PA and SA with the exception of the temperature response of monocultured PA. We studied metabolic and virulence changes in both species. Altered metabolic features at 39 °C included arginine biosynthesis and the periplasmic glucose oxidation in *S. aureus* and *P. aeruginosa* monocultures respectively. When PA co-cultures were exposed at 39 °C, they upregulated ethanol oxidation-related genes along with an increment in organic acid accumulation. Regarding virulence factors, monocultured SA showed an increase in the mRNA expression of the *agr* operon and *hld*, *pmsa*, and *pmsβ* genes at 39 °C. Supported by mRNA data, we performed physiological experiments and detected an increment in hemolysis, staphyloxanthin production, and a decrease in biofilm formation at 39 °C. On the side of PA monocultures, we observed an increase in extracellular lipase and protease and biofilm formation at 39 °C along with a decrease in the motility in correlation with changes observed at mRNA abundance. Additionally, we assessed host–pathogen interaction both in vitro and in vivo. *S. aureus* monocultured at 39 °C showed a decrease in cellular invasion and an increase in IL-8—but not in IL-6—production by A549 cell line. PA also decreased its cellular invasion when monocultured at 39 °C and did not induce any change in IL-8 or IL-6 production. PA strongly increased cellular invasion when co-cultured at 37 and 39 °C. Finally, we observed increased lethality in mice intranasally inoculated with *S. aureus* monocultures pre-incubated at 39 °C and even higher levels when inoculated with co-cultures. The bacterial burden for *P.*

[†]M. B. Galeano, A. Luqman, M. M. Ricardi, and F. Serral contributed equally to this work.

*Correspondence:

P. M. Tribelli

paulatrib@qb.fcen.uba.ar

Full list of author information is available at the end of the article



aeruginosa was higher in liver when the mice were infected with co-cultures previously incubated at 39 °C comparing with 37 °C.

Conclusions Our results highlight a relevant change in the virulence of bacterial opportunistic pathogens exposed to fever-like temperatures in presence of competitors, opening new questions related to bacteria-bacteria and host-pathogen interactions and coevolution.

Keywords Interaction, Temperature, Virulence, *Pseudomonas aeruginosa*, *Staphylococcus aureus*

Background

Pseudomonas aeruginosa and *Staphylococcus aureus* are two opportunistic bacterial species globally distributed [1, 2], which cause a variety of infections ranging from mild to severe, including skin and respiratory infections [3, 4]. Additionally, these bacteria are a major cause of both morbidity and mortality in cystic fibrosis patients, causing acute and chronic infections that lead to severe respiratory damage and (or perhaps due to) a continuous inflammatory response.

The interaction between *S. aureus* and *P. aeruginosa* has been recently reviewed [5], and it is traditionally described as antagonistic due to the secretion of different anti-staphylococcal factors by *P. aeruginosa*. Among these factors, the extracellular protease LasA affects the cell wall of *S. aureus*, leading to cell lysis, and rhamnolipids cause biofilm dispersion. *S. aureus* is sensitive to respiratory inhibitors secreted by *P. aeruginosa* such as the pigment pyocyanin, quinoline N-oxides, and cyanhydric acid which inhibit *S. aureus* respiratory chain affecting [6] the cytochrome bd quinol oxidase, which oxidizes ubiquinol and reduces oxygen as a part of the electron transport chain [7].

Despite this disadvantage, in co-culture with *P. aeruginosa*, *S. aureus* changes its metabolism to a fermentative state leading to the formation of small colony variants (SCVs). In this state, *S. aureus* is resistant to pyocyanin and cyanide and able to survive in co-culture with *P. aeruginosa*. *S. aureus* cells can also shift to L-forms to escape the cell wall lytic activity of LasA [8, 9]. However, during the last years, the coexistence of both bacteria has also been detected in cystic fibrosis patients and in vivo experiments, revealing even a cooperative interaction [10–12]. Although the interaction between both bacteria has been less explored under low oxygen conditions [9–11], microaerobiosis is relevant in cystic fibrosis and other pulmonary diseases due to the presence of mucus and oxygen gradients [13]. In this context, Pallet et al. [14] reported that anoxia leads to a phenotype of *P. aeruginosa* that is less dominant over *S. aureus*.

Besides oxygen and nutrients, another key factor for bacterial survival and physiology is temperature [15, 16]. Particularly, pathogenic species display virulence factors depending on several factors, including the host

temperature [17, 18]. Previous studies have analyzed the effects of temperature transitions from the environment to the host on *S. aureus* and *P. aeruginosa* physiology by using transcriptomic and physiological approaches [19, 20]. In bacteria, the main temperature-sensing mechanisms are RNA thermometers, which regulate the expression of genes at the post-transcriptional level through structured RNAs [18]. RNA thermometers regulate different physiological features like the virulence factor *tviA* in *Salmonella typhi* or the type three injectisome in *Yersinia pseudotuberculosis* [18, 21, 22]. Temperature-dependent traits, mainly associated with virulence, host colonization, and survival, have been recently reviewed in *Pseudomonas* spp., including *P. aeruginosa* [23].

The infection process and outcome depend on several factors, including the availability of nutrients, the micro-environment, the organ structure, and the immune host response [24–26]. Temperature is a physical factor that affects cellular physiology in the environment and during infection [27]. Pyrexia or fever is the increase in the body temperature above a specific set-point controlled by the hypothalamus [28]. This increase is often due to infection or other non-infectious causes such as inflammation or malignancy [28]. In humans, fever-like temperatures have been classified as low-grade (37.3 to 38.0 °C), moderate-grade (38.1 to 39.0 °C; used in this work), high-grade (39.1 to 41 °C), and hyperthermia or hyperpyrexia when the temperature increases above 41 °C [29]. In the context of infections, fever is considered a beneficial process for the host [30, 31]. For example, in three different *Salmonella enterica* serovars, fever-like temperatures impair infective characteristics, suggesting that fever is a signal for a persistent state [32]. In *S. aureus* USA300 strain AH1263, Bastok et al. [20] analyzed three different temperatures, including extreme pyrexia but focusing on the differences between 34 and 37 °C under aerobic conditions.

The aim of the present study was to analyze the effect of fever-like temperatures (39 °C) on the interaction between *S. aureus* and *P. aeruginosa* by using a sequential culture scheme to analyze the RNA expression profile in vitro as well as virulence traits both in vitro and in a mouse model. Our data supports that fever-like temperatures increase virulence in vitro and in vivo, particularly when *S. aureus* and *P. aeruginosa* are co-cultured.

Results

S. aureus and *P. aeruginosa* survival in co-cultures under microaerobic conditions and fever-like temperatures

We first investigated bacterial survival in microaerobic monocultures and co-cultures by using KNO_3 as an alternative electron acceptor to oxygen. The cultures were incubated at 37 °C either for 4 h (herein called 37 °C) or for 2 h, followed by incubation at 39 °C for 2 h (herein called 39 °C) (Fig. 1). We analyzed both temperature and co-culturing for both SA (Fig. 2A) and PA (Fig. 2B). We found that SA survival depends on the presence of the competitor, being significantly lower when co-cultured with PA. The observed effects are independent of temperature variations, with no additional impact. All the other comparisons showed no significant differences. Additionally, competence, determined by PA's growth inhibition of SA, was also unaffected by temperature according to plate competence assays (Fig. 2C).

Additionally, we investigated whether longer co-culture times could cause a different physiological response at 39 °C compared to 37 °C. Thus, we cultured SA, PA, and PA-SA at 37 and 39 °C in the same microaerobic conditions but for 24 h. Surprisingly, co-cultures showed an evident, blue/green-colored medium typical of pyocyanin production but only at 39 °C (Additional file 1: Fig. S1A). More intriguing is the similar CFU count in the co-cultures after 24 h at both 39 and 37 °C, despite the different pyocyanin content (Additional file 1: Fig. S1B). However, as fever nowadays lasts

for shorter periods due to antipyretic usage, we proceeded with the experimental scheme shown in Fig. 1.

Gene expression profile of *S. aureus* and *P. aeruginosa* after exposure to fever-like temperatures in different culture conditions

To investigate how these bacterial species adapt their physiology to fever-like temperatures, we next carried out total RNAseq experiments and physiological assays for SA and PA monocultures and SA-PA co-cultures, following the same culture scheme described above (Fig. 1). We analyzed the data using different approaches, including the detection of differentially expressed genes (Additional file 1: Fig. S2 and S3), using Rockhopper software (Fig. 2D) and classified the genes by their cellular function (Additional file 1: Fig. S4 and S5 and Additional file 2: Table S1 Additional file 3: Table S2).

We performed pairwise comparison of the gene expression profiles for both PA and SA comparing the following conditions: SA or PA monocultures at 39 and 37 °C (herein called mono 39 vs 37), SA or PA co-cultures and monocultured at 37 °C (further called co vs mono 37), SA or PA co-cultures and monocultured at 39 °C (further called co vs mono 39), and co-cultures at different temperatures (herein called co 39 vs 37). Overall, our results summarized in Fig. 2D showed a strong transcriptional change for most of the conditions. The only exception was monocultured PA that showed minimal change upon temperature treatments (only the 0.5% of total expressed genes showed differential expression). This finding

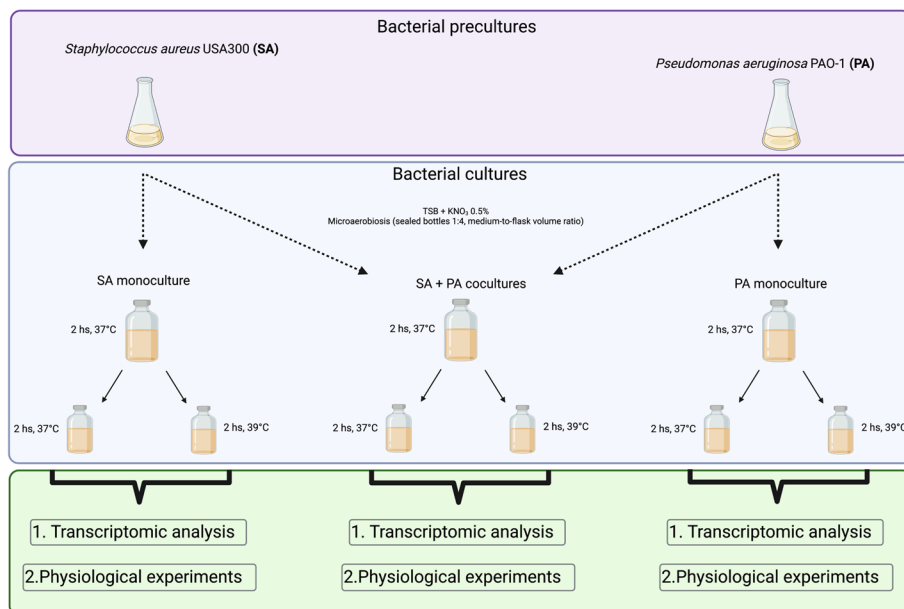


Fig. 1 Culture conditions and experimental design. Experimental scheme to analyze the effect of fever-like temperatures on the physiology and interaction of *S. aureus* USA300 (SA) and *P. aeruginosa* PAO1 (PA)

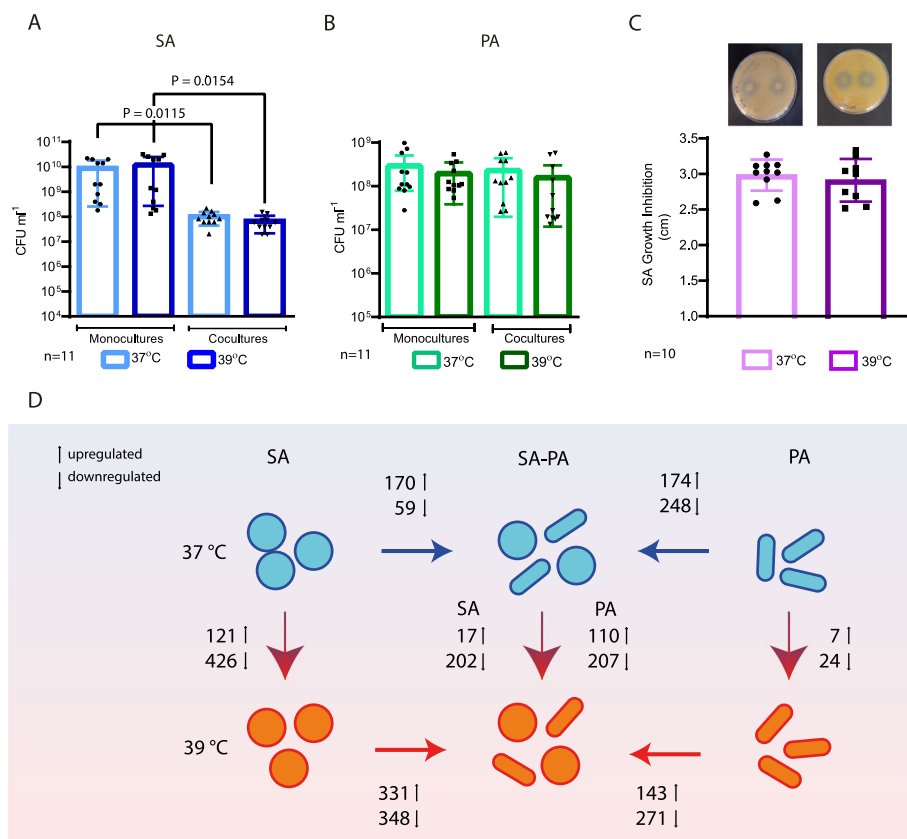


Fig. 2 Survival and competence assays. SA and PA were cultured under microaerobic conditions either at 37 or 39 °C following the scheme shown in Fig. 1, in mono- or co-culture, and survival was measured as CFU/ml on selective media. **A** SA count was determined on TSA + NaCl plates (1-way ANOVA, only statistically significant comparisons shown). **B** PA was determined on cetrимide plates for PA (1-way ANOVA, non-significant). **C** Competence test in agar plates performed as described in “Methods” (unpaired *t*-test, non-significant). **D** Summary of the differential expressed gene number obtained by RNAseq experiments across different culture and temperature conditions

strongly contrasted with the sharp response of co-cultured PA to fever-like temperatures (Fig. 2D).

Additionally, we performed a principal component analysis (PCA) (Additional file 1: Fig. S6A and B). For SA, the PCA showed that the first PC discriminated between culture condition (mono or co), while the grouping by temperature was less evident in any of the first three components (Additional file 1: Fig. S6A). The first and second components explained 89.8% of the data variation (Additional file 1: Fig. S6A) for SA and 88.6% for PA (Fig. S6B).

Metabolic reshaping of *S. aureus* monocultures after exposure to fever-like temperatures

We also performed a Gene Ontology Enrichment (GOE) analysis, which allows the detection of a global trend of the metabolic pathway or branch over-represented within the differentially expressed genes, even if not all the genes involved present significant differences in the RNAseq analysis (Additional file 4: Table S3 and S4). The

GOE analysis in the SA mono 39 vs 37 expression dataset showed an enrichment in the arginine, tricarboxylic acid (TCA) cycle, and fermentative pathways (Tables S1 and S3).

Particularly, we found that some genes related to arginine metabolism were upregulated at 39 °C (Fig. 3A, Additional file 2: Table S1, Additional file 4: Table S5). To test if temperature affects arginine metabolism, SA monocultures were grown in complete defined medium (CDM) supplemented with glucose and KNO₃ but without arginine or proline, following the same temperature scheme as that described above. Results showed that bacterial count in glucose-supplemented medium without arginine or proline was higher at 39 °C than at 37 °C (Fig. 3B), supporting the RNAseq observations and suggesting that arginine biosynthesis is triggered by fever-like temperatures.

Regarding the TCA cycle pathway, we found that genes were upregulated at 39 °C along with genes related with peripheral feeding pathways (Fig. 4A, Additional file 2:

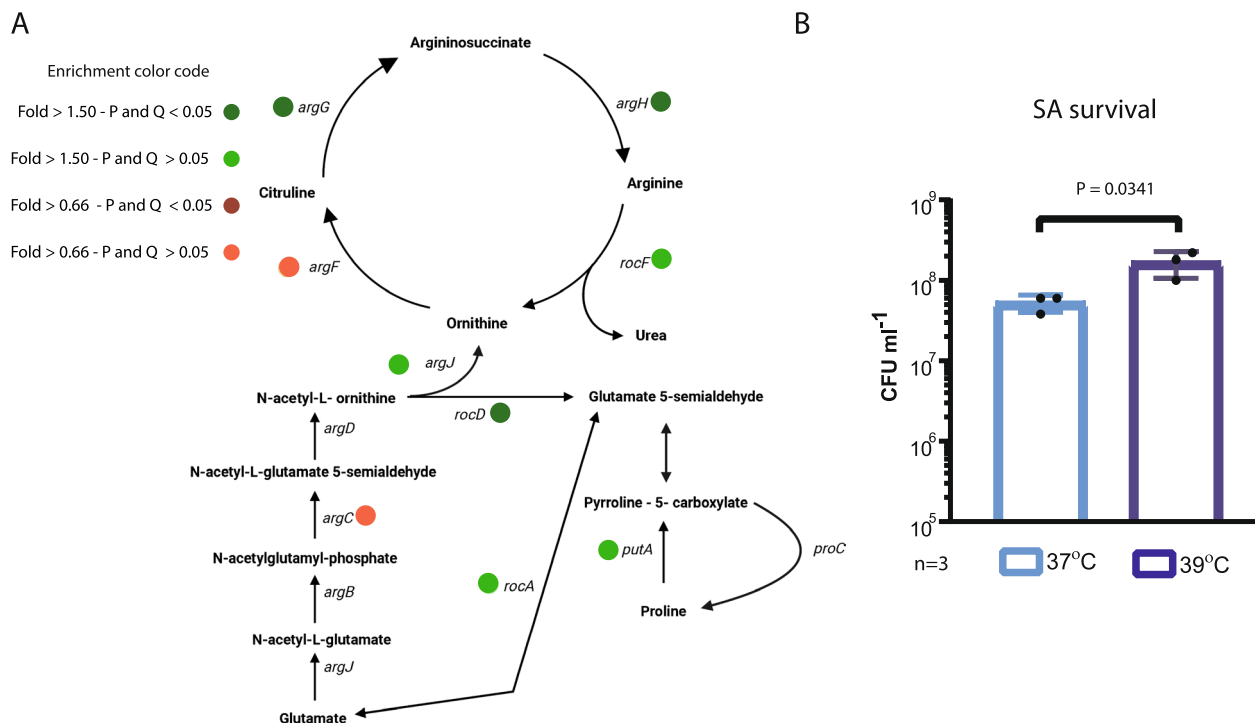


Fig. 3 **A** Effects of temperature and culture conditions in SA arginine metabolism. Schematic overview of arginine biosynthesis and degradation metabolism in SA. Genes with changes at 39 °C (both with a significant difference or a non-significant trend are indicated with color coded spots on the figure). **B** SA survival in CDM medium lacking arginine and proline and supplemented with 0.5% KNO₃. Cultures were incubated under microaerobiosis for 2 h at 37 °C and further split and incubated at 37 or 39 °C for 2 h. CFU/ml was determined on TSA agar plates and compared by unpaired *t*-test

Table S1, Additional file 4: Table S5). On contrary, genes encoding proteins related to fermentation branches were in general downregulated at 39 °C (Fig. 4A, Additional file 2: Table S1, Additional file 4: Table S5) except for the upregulation of the *fdhD* gene encoding the formate dehydrogenase subunit. Additionally, the expression of *fdh* and *fdhA* genes increased, though non-significantly (Additional file 2: Table S1, Additional file 4: Table S5).

Although the cultures were incubated under microaerobic conditions in the presence of nitrate, genes encoding the respiratory nitrate reductase and the responsive nitrogen regulation system NreABC, which activates nitrate and nitrite dissimilation [33], were downregulated in mono 39 vs 37 along with nitrite reductase genes which catalyzed a reaction not coupled with energy production (Fig. 4A, Additional file 2: Table S1, Additional file 4: Table S5). In concordance with the gene expression profile, nitrite accumulation in the supernatant of SA monocultures was significantly decreased at 39 °C as compared to 37 °C (Fig. 5A) [33]. In SA monocultures at 39 °C, the expression of cytochrome D ubiquinol oxidase coding genes were repressed, while the rest of the genes encoding cytochrome subunits were similarly expressed at 39 and 37 °C (Additional file 1: Fig. S7A,

Additional file 2: Table S1, Additional file 4: Table S5). Additionally, when we investigated organic acid production in SA monocultures in CDM supplemented with glucose at 37 and 39 °C under microaerobic conditions by high-performance liquid chromatography (HPLC), we detected a decrease in succinate accumulation in the culture supernatant, but an increase in formate at 39 °C vs 37 °C, while the rest of the organic acids were similar between temperatures (Fig. 5B).

The integration of these results suggests that SA monocultures feed the TCA cycle at 39 °C through α -ketoglutarate to obtain energy, probably through cytochrome quinol and the succinate oxidase complex (Fig. 4A).

***P. aeruginosa* gene expression profile in monocultures and metabolic features after fever-like temperature exposure**

The few changes observed in PA monocultures after treatment with fever-like temperatures included the upregulation at 39 °C of an operon reported as iron responsive [34] including *fumC1*, which encodes a fumarate reductase and *sodM*. On the contrary, another key *Pseudomonas* metabolic pathway, the periplasmic

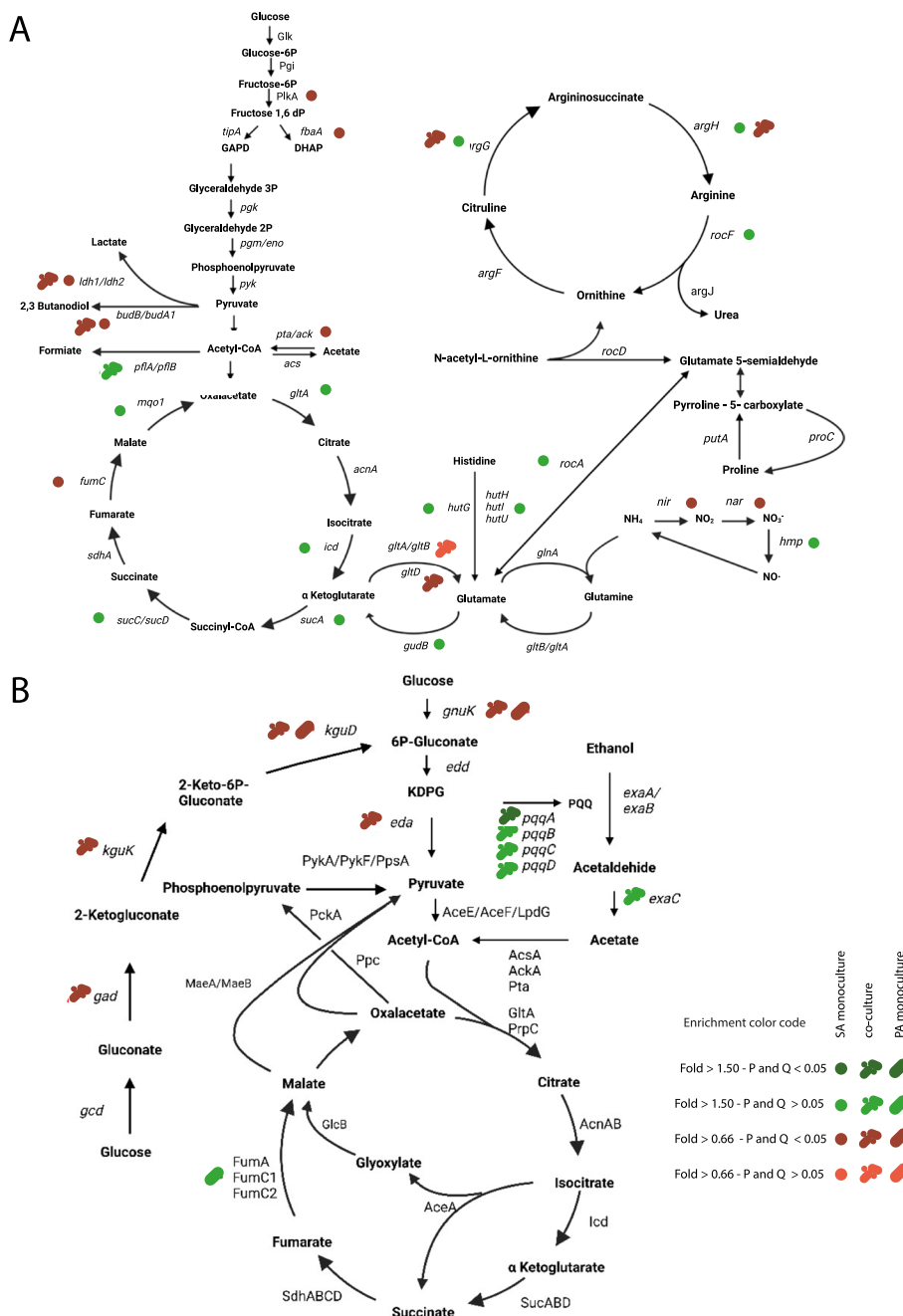


Fig. 4 Effects of temperature and culture conditions in SA and PA central metabolic pathways. **A** Schematic overview of SA carbon central metabolic pathways for monocultures 39 vs 37 °C and co-cultures 39 vs 37 °C. **B** Schematic overview of PA carbon central metabolic pathways for monocultures 39 vs 37 °C and co-cultures 39 vs 37 °C

glucose oxidation, was repressed at 39 °C, with almost all the genes repressed (*kgut*, *kguk*, *kgD*, and *kgnt*) (Fig. 4B, Additional file 3: Table S2, Additional file 4: Table S4, Table S6).

Nitrite production was similar for PA monocultures incubated at both temperatures (Fig. 5A) while in the Durham tube assay, gas production after 48 h was lower

at 39 °C, although growth was similar to that observed at 37 °C (Fig. 5C). The organic acid profile in CDM supplemented with KNO₃ and glucose showed a low concentration of organic acids in the supernatants of PA monocultures, particularly acetate (Fig. 5B). Cytochrome expression showed no significant differences between temperatures (Additional file 3: Table S2, Fig. S7B).

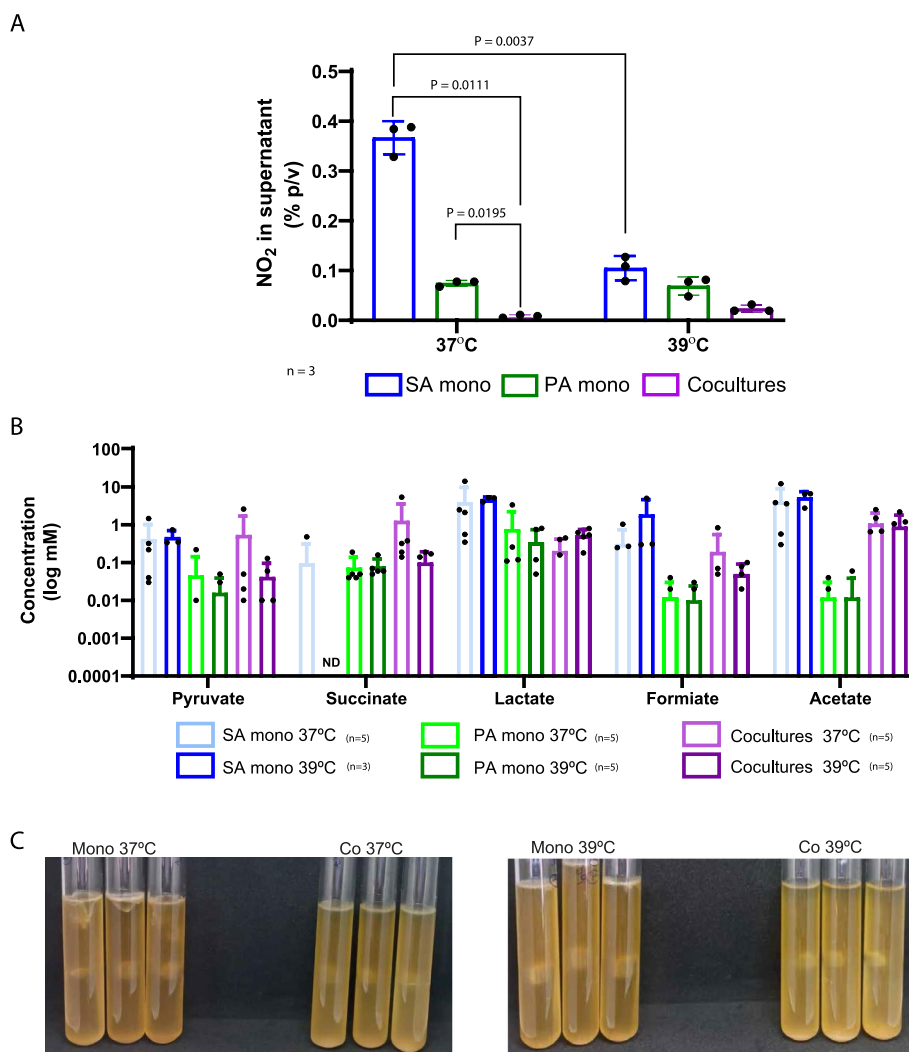


Fig. 5 Nitrite production, organic acid content, and denitrification in SA and PA monocultures and co-cultures at different temperatures. **A** Nitrite production in SA and PA monocultures and co-cultures at 37 and 39 °C as described in Fig. 1. Nitrite concentration in the supernatant was determined using the colorimetric Griess assay. Only significant differences are displayed with their corresponding *P*-value after using 2-way ANOVA, Tukey's multiple comparisons test. **B** Organic acid content in the culture supernatant was determined by HPLC in CDM cultures supplemented with glucose and 0.5% of KNO₃. Cultures were incubated following the scheme shown in Fig. 1. **C** Denitrification assay using Durham tubes. Monocultures and co-cultures were performed in TSB + KNO₃ (0.5%) and incubated at 37 or 39 °C for 48 h and bubble size was observed

Culture condition impacts on bacterial physiology depending on temperature

For SA in co vs mono at 37 °C, the GOE analysis showed five over-represented categories, including purine metabolism, amino acid biosynthetic and catabolic processes, siderophore biosynthesis, and heme transport (Additional file 4: Table S3). The heme degradation and staphyloferrin B biosynthesis pathways were also represented among the upregulated genes in co-cultures, when compared with monocultures at 37 °C (Additional file 2: Tables S1, Additional file 4: Table S3, Table S5). Particularly, enrichment in the biosynthetic amino acid

pathways for L-isoleucine, L-valine and L-leucine were over-represented, with genes belonging to this metabolism upregulated in SA co-cultures (Additional file 2: Table S1, Additional file 4: Table S3, Table S5). In micro-aerobic co-cultures, SA displayed fermentative metabolism with Ldh and Pfl coding genes upregulated in co-cultures (Additional file 2: Table S1, Additional file 4: Table S3, Table S5).

In the same comparison (co vs mono 37), PA genes involved in the peripheral fructose catabolic pathway were repressed (Additional file 3: Table S2, Additional file 4: Table S4, Table S6). Additionally, the GOE analysis

showed enrichment in cysteine metabolism, with upregulated genes belonging to the assimilatory sulfonate reduction superpathway (Additional file 3: Table S2, Additional file 4: Table S4, Table S6).

RNAseq analysis of co vs mono 39 for SA showed upregulation in several glycolysis-related genes (Additional file 2: Table S1, Additional file 4: Table S3, Table S5) and staphyloferrin biosynthesis genes. Interestingly, TCA-enzyme-coding genes and three succinate dehydrogenase subunits coding genes were repressed (Additional file 2: Table S1, Additional file 4: Table S3, Table S5). Concomitantly, genes related with fermentation *pflA*, *pflB*, and three genes encoding lactate dehydrogenase showed a strong expression increase ranging from 121 to fourfold in co vs mono 39 (Additional file 2: Table S1, Additional file 4: Table S5).

The PA expression profile in the same conditions (co vs mono 39) revealed repressed genes that belong to the periplasmic glucose oxidation pathway (Additional file 3: Table S2, Additional file 4: Table S4, Table S6). In contrast, we found overexpression of genes belonging to glyoxylate shunt and of genes encoding the succinate dehydrogenase subunits (Additional file 3: Table S2, Additional file 4: Table S4, Table S6), suggesting that in PA, glyoxylate could feed the TCA cycle through succinate in co vs mono 39. Moreover, genes encoding a L-lactate dehydrogenase (that oxidizes L-lactate) and permease were upregulated in co vs mono independently of temperature, but with a sharper effect at 39°C (3.6 and sevenfold for mono vs co 37 and 7 and 20-fold for co vs mono 39, respectively) (Additional file 3: Table S2, Additional file 4: Table S6). In concordance with lactate consumption, we detected lower lactate levels in co-culture supernatants compared with monocultures (Fig. 5B).

Fever-like temperatures affect *S. aureus* and *P. aeruginosa* gene expression profile in co-cultures

When we compared co-cultures at different temperatures (co 39 vs 37), we observed the repression of genes belonging to transcription and translation processes as well as envelope modification, and of the enterotoxin-coding genes *seq* and *sek* at 39 °C for SA (Additional file 2: Tables S1 and Additional file 4: S3). In contrast, only genes comprising the PTS type II ascorbate-specific operon were upregulated at 39 °C (Table S1). In general, when PA was present, SA central metabolic genes were not affected by temperature. Some exceptions were *ldh*, *budB*, and the cytochrome D ubiquinol oxidase subunits, which were downregulated at 39 °C (Additional file 1: Fig. S7A, Additional file 2: Table S1, Additional file 4: Table S5).

For PA, co 39 vs 37 expression profile analysis showed changes in key metabolic features. Genes belonging to the ethanol oxidation pathway, which is a secondary

metabolic branch present in *Pseudomonas* species for energy production through oxidation of ethanol [35], were upregulated at 39 °C (Fig. 4B, Additional file 4: Table S6). These included genes belonging to the PQQ biosynthesis, an iron-containing aldehyde dehydrogenase, the cytochrome C, and the response regulator *erbR* (Fig. 4B, Additional file 1: Fig. S7B, Additional file 3: Table S2, Additional file 4: Table S6). Genes related to anaerobic metabolism were repressed in co-cultures at 39 °C in comparison with 37 °C, even when both were incubated under low oxygen conditions in the presence of nitrate (Additional file 3: Table S2, Additional file 4: Table S6). Accordingly, nitrite accumulation in co-cultures was similar at both temperatures and lower than in monocultures after 4 h of incubation (Fig. 5A). Gas accumulation in Durham tubes after 48 h showed a similar bubble size and similar growth when comparing co 39 vs 37, but smaller when compared with monocultures (Fig. 5C). Comparing co 39 vs 37 organic acid content in the whole supernatant pyruvate, succinate and formate content was decreased (Fig. 5B).

Temperature has a different impact on *S. aureus* but not *P. aeruginosa* depending on the culture conditions

We additionally performed a multifactorial ANOVA for each gene present in the RNAseq with false discovery rate (FDR) correction method to understand if there were interactions between temperature and culture conditions (mono or co). We found no statistical interaction between the culture condition and temperature for PA (Additional file 1: Fig. S8A). In contrast, for SA, this analysis showed an interaction between these factors for a gene set crucial for SA virulence, the *agr* operon (Additional file 1: Fig. S8B; Additional file 4: Table S7). In SA monocultures, the *agrABCD* operon was overexpressed at 39 °C in comparison with 37 °C (four-fold on average, Additional file 2: Table S1). As expected, *agr* overexpression caused an increase in the expression of its direct target genes *psmβ1*, *psmβ2*, and *hld* as well as other direct and indirect targets (Fig. 6A, Additional file 2: Table S1). The opposite effect was detected in co vs mono 39 where the *agr* operon was repressed (Fig. 6A, Additional file 2: Table S1) while its direct targets showed different pattern. When we compared the SA expression profile of co 39 vs 37, or co vs mono 37, we did not find differences in *agr* genes or its targets (Fig. 6A).

Fever-like temperatures trigger virulence factors and alter antibiotic resistance in *S. aureus* and *P. aeruginosa* in vitro

Considering the impact of fever-like temperature (39 °C) on gene expression, we tested its impact on other virulence factors of SA monocultures in vitro, including DNase activity, pigment production, hemolysis, biofilm

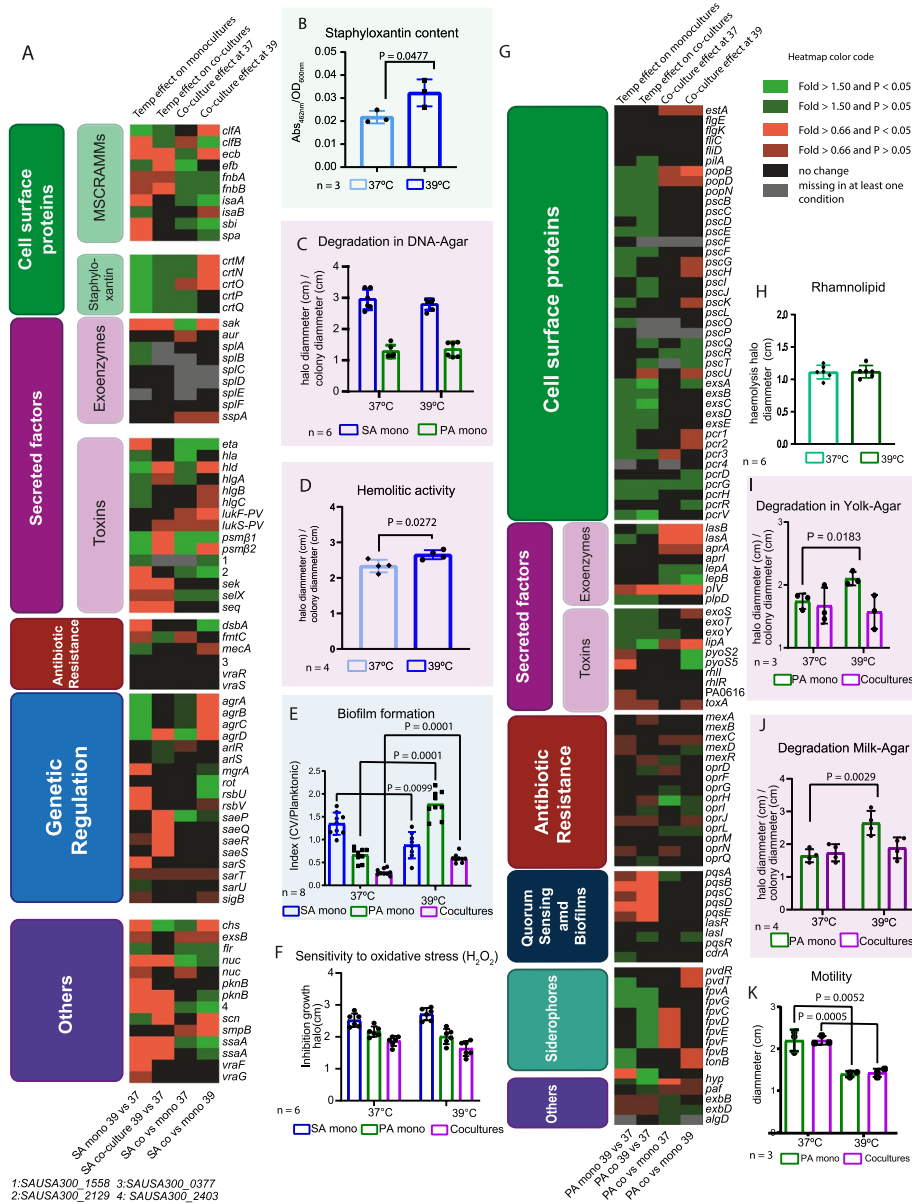


Fig. 6 Fever-like temperatures trigger virulence factors and alter antibiotic resistance in both SA and PA. **A** Heat map representing the gene expression profile of SA cultured in different conditions and temperatures. **B** Staphyloxanthin production after incubating SA in monoculture following the scheme described in Fig. 1. Methanol-extracted pigment from supernatants was measured at 462 nm. **C** Extracellular DNase activity (degradation halo) for SA or PA monocultures assayed in DNA-agar plates incubated overnight at 37 or 39 °C. **D** SA extracellular hemolytic activity tested in sheep blood agar plates inoculated with SA monocultures incubated overnight at 37 or 39 °C. Clear halo and the colony diameter are informed. **E** Biofilm formation in multiwell plates with SA monoculture incubated overnight at 37 or 39 °C. Biofilm formation index was calculated as crystal violet (CV) $\lambda_{570\text{ nm}}$ /planktonic cells $\lambda_{595\text{ nm}}$ for each replicate. **F** Sensitivity to oxidative stress. Lawns of SA, PA, or co-cultures were seeded in TSA plates. A 5- μ l drop of H₂O₂ was placed in a sterile paper disc and further incubated at 37 or 39 °C. **G** Heat map representing the gene expression profile of PA cultured under different conditions. **H** Rhamnolipid production in PA monocultures was determined by the hemolytic halo in sheep blood agar plates incubated at 37 or 39 °C. **I** Lipase extracellular activity in egg-yolk-supplemented TSA plates incubated at 37 or 39 °C. Clear zones or white precipitates were determined. **J** Protease extracellular activity in milk-supplemented TSA plates incubated at 37 or 39 °C. The clear zone and colony diameter were determined. **K** Motility of PA mono- and co-cultures was analyzed in motility plates incubated at 37 or 39 °C. All diameter measurements were performed with the ImageJ software. Individual values for each measurement are shown. An unpaired *t*-test was performed, and only significant differences are informed with their corresponding *P*-value

formation, and colony phenotype in Red Congo agar [36, 37].

In vitro staphyloxanthin production was higher at 39 °C (Fig. 6B), in concordance to the biosynthetic operon staphyloxanthin being overexpressed at that temperature (Fig. 5A, Additional file 2: Table S1, Additional file 4: Table S5). Extracellular DNase activity in DNA agar plates was similar at both temperatures after 24 h of incubation (Fig. 6C, Additional file 4: Fig. S9A). We also tested the colony phenotype in Congo red plates, where SA presented similar, black-pigmented colonies both at 37 and 39 °C (Additional file 1: Fig. S9B). Hemolysis, as tested in blood agar plates, was higher at 39 °C (Fig. 6D, Additional file 1: Fig. S9C). Biofilm formation, as assayed in polystyrene multiwell plates using TSB medium supplemented with KNO₃, was lower at 39 °C, in line with our RNAseq data (Fig. 6E) and with the upregulation of *agr* under the same conditions [38].

Antibiotic resistance was screened using the Sensititre plate multi-test for *S. aureus* monocultures incubated at 37 or 39 °C during the entire test. We found that in general the antibiotic resistance was similar in SA monocultures except for moxifloxacin and daptomycin that presented a onefold increase in the Minimal Inhibitory Concentration (MIC) at 39 °C compared with those obtained at 37 °C (Additional file 4: Table S8). Additionally, we found no differences in the oxidative stress resistance assay for SA monocultures incubated at different temperatures (Fig. 6F).

For PA mono 39 vs 37, RNAseq analysis related to the virulence factors, summarized in Fig. 6G, showed that genes related to the quorum sensing *pqs* system were repressed at 39 °C. In PA monocultures, extracellular DNase activity, lipase and rhamnolipid production were similar at both temperatures (Fig. 6B, I, and H, Additional file 1: Fig. S8A and C). Extracellular protease activity of PA monocultures at 39 °C was significantly higher while motility was lower (Fig. 6J and K, Additional file 1: Fig. S8D and E). Antibiotic resistance at different temperatures was also tested using the Sensititre panel for Gram negative bacteria. We showed a twofold decrease in cefotaxime MIC and an increase in minocycline resistance at 39 °C (Additional file 4: Table S9). Oxidative stress resistance showed similar results at both temperatures (Fig. 6F).

In co-cultures, the PA type III secretion system (TSS3) regulators *exsA* and *exsC* and TSS3 related *pcrV* were upregulated at 39 °C, other related genes showed the same trend albeit non-statistically significant (Fig. 6G, Additional file 3: Table S2). The phenazine production genes and the extracellular lipase coding gene *lipA* followed the same trend, being upregulated at 39 °C (Fig. 6G, Additional file 3: Table S2). Considering these

changes, we tested the extracellular lipase activity in co-cultures and observed higher activity at 39 °C while extracellular protease activity showed similar results at both temperatures (Fig. 6I, J, Fig. S8 C and D). Motility, which is mostly driven by PA, decreased at 39 °C in co-cultures, similar to what was found in monocultures, thus showing a temperature effect despite the presence of SA. When we compared the expression of SA virulence factors at co 39 vs 37, we found repression at 39 °C of the Sae regulon, *nuc*, *sek*, *seq*, *ecb*, *efb*, *pknB*, *scn*, *sak*, *agrD*, and two direct targets of the *agr* system *psmβ1* and *psmβ2* (Fig. 6A).

Temperature affects SA- and PA-induced cytokine production and invasion in human cell lines

To further investigate these in vitro observations, we analyzed cytokine production and cellular invasion on the epithelial lung cell line A549. Cells were infected with inoculum grown following the same culture scheme described in Fig. 1. When A549 cells were infected with PA monocultures, production of the IL-8 and IL-6 cytokines was similar despite temperature (Fig. 7A, B). Contrarily, A549 cells infected with SA monocultures at 39 °C exhibited higher pro-inflammatory IL-8 production compared to those infected with SA monocultures at 37 °C, with IL-6 production remaining similar at both temperatures (Fig. 7A, B).

When cells were infected with SA-PA co-cultures, a similar production of IL-6 and IL-8 was observed regardless of the temperature, although a slight increment was observed for IL-8 production at 39 °C (Fig. 7A, B). Additionally, IL-6 production was lower when A549 cells were infected with co-cultures comparing with PA monocultures at both temperatures (Fig. 7B).

When the cellular invasion assays were performed with SA monocultures incubated at 39 °C, a decrease in cellular invasion was observed, in agreement with a more virulent profile (Fig. 7C). In contrast, cellular invasion for SA in co-cultures showed no differences between temperatures (Fig. 7C). However, for PA in co-cultures, we found a decrease in cellular invasion at 39 °C comparing with 37 °C (Fig. 7C). Overall, our results show that fever-like temperature affects SA virulence, suggesting an acute infective state when PA is absent and a contrary effect upon its presence.

Serum albumin is a major protein in plasma that affects gene expression, virulence, and survival in other pathogens like *Acinetobacter baumannii* [39, 40]. We assessed human serum albumin (HSA) effect on monocultured or co-cultured PA or SA at 37 or 39 °C following the same culture scheme (Fig. 1) but in the presence or absence of this protein.

We did not find any effect of the HSA for any of the treatments (Fig. 7D).

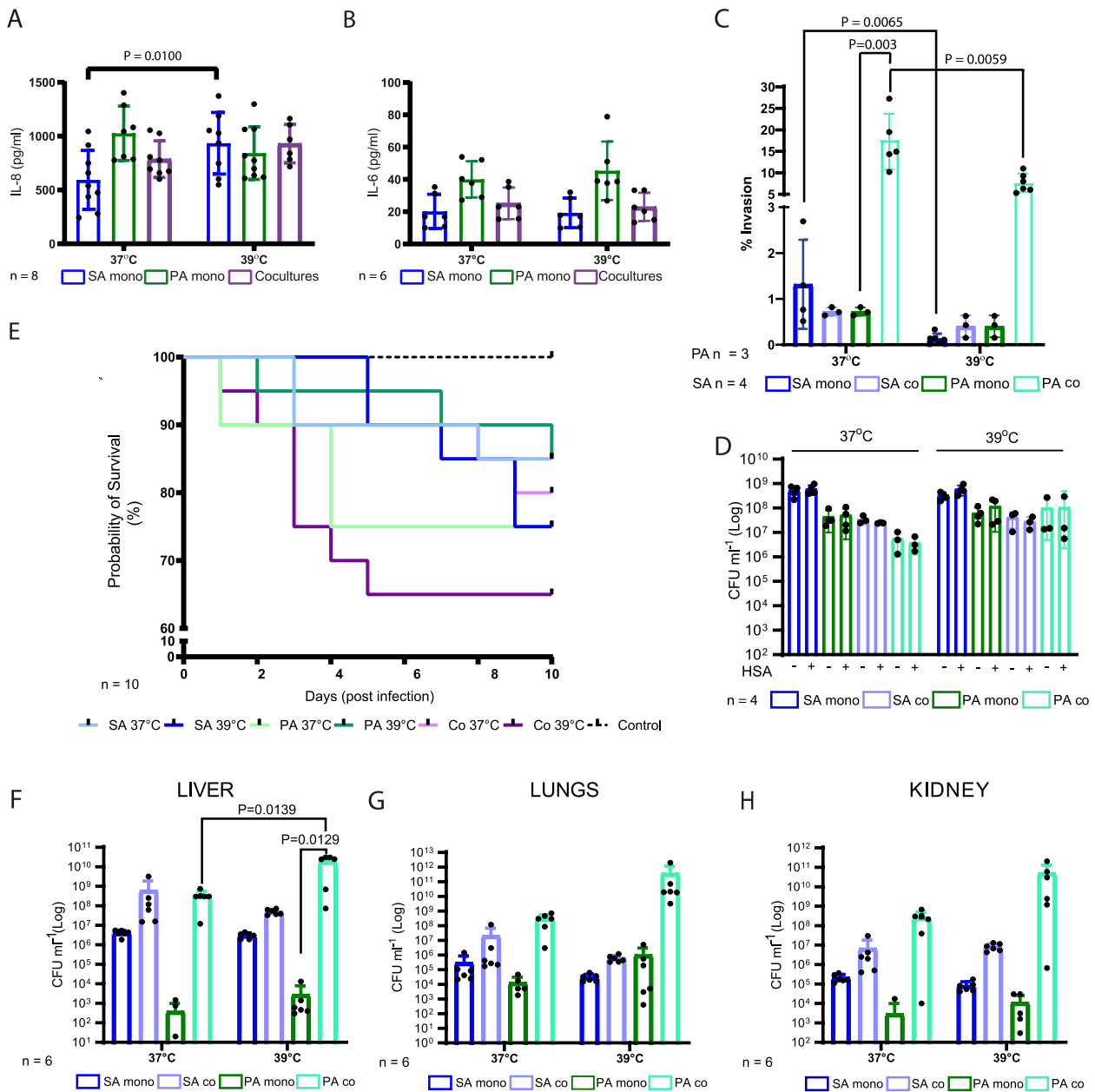


Fig. 7 Fever-like temperatures impact on inflammatory cytokine production, cellular invasion, and in vivo virulence. **A** Production of IL-8 in the A549 cell line. **B** Production of IL-6 in the A549 cell line. **C** Invasion assay in A549 cell lines infected with bacterial cultures prepared as was shown in Fig. 1. Results are presented as percentage of bacterial inoculum that was internalized. The results were analyzed for each microorganism separately. The graph displays two different scales for better visualization. **D** Effect of human serum albumin on SA and PA survival at 37 or 39 °C. **E** Mouse survival was evaluated using 10 individuals for each group intranasally inoculated with mono- or co-cultures incubated as described in Fig. 1. Sterile PBS was used as a negative control. Mouse survival was monitored daily for 10 days. The graph has a scale break for better data visualization. **F** Bacterial burden in the liver. **G** Bacterial burden in the lungs. **H** Bacterial burden in the kidney. Zero values obtained in the bacterial count are not shown on the Log scaled graphs but mentioned on the graph and were considered for statistical analysis. Zero values included (non-infected control $n = 6$ for all organs; PA mono 37 $n = 1$ in liver; $n = 1$ in lungs and $n = 5$ in kidney; PA mono 39 presented zero values in $n = 1$ in kidneys). **A–C, H** Two-way ANOVA, **E, G** 1-way ANOVA, Sidak’s multiple comparisons test. Only significant differences were displayed with their corresponding P -value

In vivo virulence is affected by temperature and culturing in a mouse model

We next performed intranasal infections in mice with bacteria cultured as we described in Fig. 1. We used this simplified model in which the bacteria were previously exposed to different temperatures to understand how this factor impacts on bacterial virulence. We tested both mouse survival and bacterial burden in the mouse lungs, kidneys, and liver. Although there were not significant differences at the end of the experiment, we observed that survival was lower when mice were infected with SA monocultures pre-incubated at 39 vs 37 °C (Fig. 7E). In contrast, when mice were infected with PA monocultures, mouse survival was lower when the inoculum was grown at 37 °C (Fig. 7E). Moreover, SA-PA co-cultures incubated at 39 °C caused greater mortality than those incubated at 37 °C, and this was the treatment that caused the highest mortality in mice (Fig. 7E).

Bacterial burden in the lungs, kidneys, and liver showed that SA count in these organs was similar when comparing between temperatures but was slightly higher when SA was in co-culture (Fig. 7 F–H). For PA, we showed that in liver bacterial burden was significantly higher when we compared co-cultures and monocultures at 39 °C (Fig. 7F–H). Importantly, PA co-cultures led to significantly higher counts in liver at 39 °C than at 37 °C and in kidney and lungs we also observed the same trend although the differences were not significant (Fig. 7 F, G and H).

Discussion

Fever is considered beneficial for infection resolution and host survival, and it is part of the acute phase response. Antipyretic treatments can increase mortality in influenza patients [41, 42]. Evans et al. (2015) outlined fever's contributions to infection control, including enhanced bacterial lysis by serum components and immune system stimulation [42]. However, host–pathogen coevolution suggests the selection of bacterial features countering fever effects.

The effect of temperature has been studied mostly as a signal indicating the shift from the environment to the host. When temperature increases from 22 to 37 °C, *P. aeruginosa* PAO1 and PA14 upregulate virulence factors like quorum sensing genes, exoproteins, and siderophores [19, 43]. For SA, Bastock et al. (2021) reported an expression profile rearrangement in SA cultures incubated at 40 °C under aerobic monocultures [20]. However, the authors exclusively conducted infection experiments on a human nasal epithelial cell line, comparing SA incubated at 34 and 37 °C. In our model, we chose a sequential 2-h incubation at 37 °C followed by 2 h at 39 °C under low oxygen conditions to understand the

early response of bacteria to the temperature shift from the host to a fever-like situation. Recently, Hamamoto et al. (2022) performed an in vivo RNAseq of *S. aureus* colonizing the mouse liver and reported that genes related to low oxygen levels are upregulated at 24 and 48 h post-infection supporting the importance of microaerobiosis used in this work [44].

In monocultures, our results showed a different response of *P. aeruginosa* PAO1 and *S. aureus* USA300 to fever-like temperature. SA monocultures showed a decrease in nitrate reduction, a decrease in the expression of genes related to fermentative metabolisms and the overexpression of arginine biosynthesis and TCA-related genes.

Reslane et al. (2022) demonstrated that SA functions as functional arginine prototroph in the absence of both glucose and arginine, being the lack of the latter insufficient to trigger arginine biosynthesis [45]. The authors propose that in abscess, arginine and glucose depletion caused by active macrophages serves as an environmental cue for SA to activate arginine biosynthesis from proline [45]. Our hypothesis is that incubation of SA at a fever-like temperature for 2 h could also serve as a cue to trigger the same prototrophy even though glucose is present. We propose that fever is also a signal to display a response to host immune system.

The most important SA in monoculture response to 39 °C was the increase in the expression of the *agr* operon and the differential expression of its direct and indirect targets along with enhanced hemolysis and staphyloxanthin production and lower biofilm formation. Our results were in line with Bastock et al. where the authors found that staphyloxanthin production increases, but in aerobic instead of microaerobic conditions, at 40 °C and only after 30 min of incubation [20]. On contrary, Palela et al. [46] reported that at 40.5 °C, hemolysis decreases because temperature affects hemolytic pore kinetics, showing the complex scenario of virulence.

Overall, our expression profile and phenotypic data suggest enhanced virulence of the bacteria pre-cultured at 39 °C. This is further supported by the host response that included increased IL-8 levels, reduced lung cell line invasion by SA, and a trend towards decreased mice survival. Considering fever as a primary non-specific immune response [47], we propose that the observed rise in virulence in SA counteracts this response, thereby promoting the infection's success.

In contrast, PA monocultures showed a different pattern characterized by a more robust metabolism, with less differentially expressed genes in response to fever-like temperatures and only some virulence features increased at 39 °C in agar plates. Accordingly, host IL-8 and IL-6 production and invasion in A549 cells were

not affected by temperature in PA monocultures. Mice survival and bacterial burden showed no significant differences. All these results suggest that fever-like temperatures would not be an important signal for PA in the competitor's absence.

The differences observed between SA and PA response in monocultures could be related to the adaptation to the host. PA is a versatile environmental bacterium that can cause opportunistic infections in immune compromised, cystic fibrosis, or diabetic patients. On contrary, SA possess a wide battery of virulence factors, immune system evasion, and even mechanisms to persist and divide inside the cells provoking frequent infections within the community, not only in immune compromised or chronic patients [48]. Under light of this, it is tempting to speculate that SA that depends more highly on its pathogenic abilities shows a strong pathogenic response to fever-like temperatures in order to successfully colonize its host while PA keeps its environmental adaptability and colonizes less challenging niches.

When it comes to co-cultured bacteria under different temperatures, the scenario is more complex. SA co-cultured with PA compared with SA in monocultures (co vs mono) showed a strong expression increase in genes encoding fermentative enzymes and a repression of TCA at 37 °C. Although a fermentative metabolism increase for SA in the presence of PA was expected, as previously reported [5], the effect was further potentiated at 39 °C (co vs mono 39). We also observed this effect across SA genes related to *ldh* gene heme degradation and staphyloferrin B biosynthesis. The significance of the two latter pathways in infections lies in their critical role in acquiring iron from heme, a primary host iron source crucial for competition with PA [49]. The upregulation of SA *ldh* would allow PA to exploit on increased lactate availability by the upregulation of L-lactate dehydrogenase and L-lactate permease coding genes. PA consumption of lactate produced by SA was reported [50], and we observed sharper differential expression of the involved genes at fever-like temperatures.

Overall, when we compared co vs mono at different temperatures, the main metabolic features were not modified; however, we found an effect of temperature on the intensity of the response to the competitor.

When we compared co-cultures at 39 and 37 °C (co 39 vs 37), we noticed different expression patterns, with few upregulated genes in SA, comprising the PTS type II ascorbate-specific operon, which has been reported to alter the properties of SA cell wall and thereby modulate virulence [37]. In contrast, PA co-cultures displayed a large number of differentially expressed genes between temperatures, being the most remarkable metabolic feature, the upregulation of genes related to ethanol

oxidation. This could be in response to SA fermentative metabolism that could lead to ethanol production.

Regarding host response, we observed a trend towards increased IL-8 production in co-cultures at 39 vs 37 °C in A549 epithelial lung cells, along with a significant increase in SA cellular invasion, independent of culture temperature. This complex scenario for coinfection was described also by Chekabab et al. only at 37 °C where the authors described an inhibitory effect of SA filtrated supernatants on IL-8 production in the airway epithelial cell line Beas-2B stimulated with *P. aeruginosa* [51]. Alves et al. reported an intermediate interleukin production by cells infected with mixed biofilms and a wound healing delay [52]. A similar effect was observed in this work but at 37 °C, while at 39 °C the IL-8 production was higher although the differences were not significant when compared with co 39 vs 37. However, PA invasion in co-cultures was significantly lower at 39 °C.

Although mice are physiologically different from humans, it is still a widely used model. In mice, hypothermia can be displayed, but also temperature rise upon infections, particularly after LPS administrated in low doses and endotoxin [53, 54]. Eskilsson et al. (2021) have recently reported that, in mice, the humoral response is implicated in eliciting fever responses during localized inflammation [55]. Due to the complex process of fever in mice, we used a simplified in vivo model in which only the bacteria were exposed to fever-like temperature to understand the early physiological response and its consequences. Our results revealed that bacteria pre-incubated at 39 °C showed a different behavior depending on the species and the culture condition (summary in Fig. 8). In monocultures, albeit not significant, a different trend was observed for SA and PA at 39 °C comparing to 37 °C. SA monocultures intranasally inoculated caused higher lethality at 39 °C in mice, with similar bacterial burden in the different organs. In contrast, PA monocultures caused a slightly lower mouse mortality.

However, the most evident in vivo effect was observed for co-cultures incubated at 39 °C. These severely impacted on mouse survival rate and led to an increase in PA bacterial burden in all the organs tested, with significant differences in liver. In contrast, for SA the results were similar and independent of the temperature but higher than those obtained with monocultures, in agreement with the cell invasion assays.

In our work, we observed that an overnight incubation of co-cultures at 39 °C lead to a blueish color, typical of pyocyanin production but with a SA CFU count similar to 37 °C co-cultures, which did not show this color. Previous reports showed that pyocyanin production is lower under microaerobiosis comparing with aerobic conditions leading to a higher coexistence with SA [12]. While

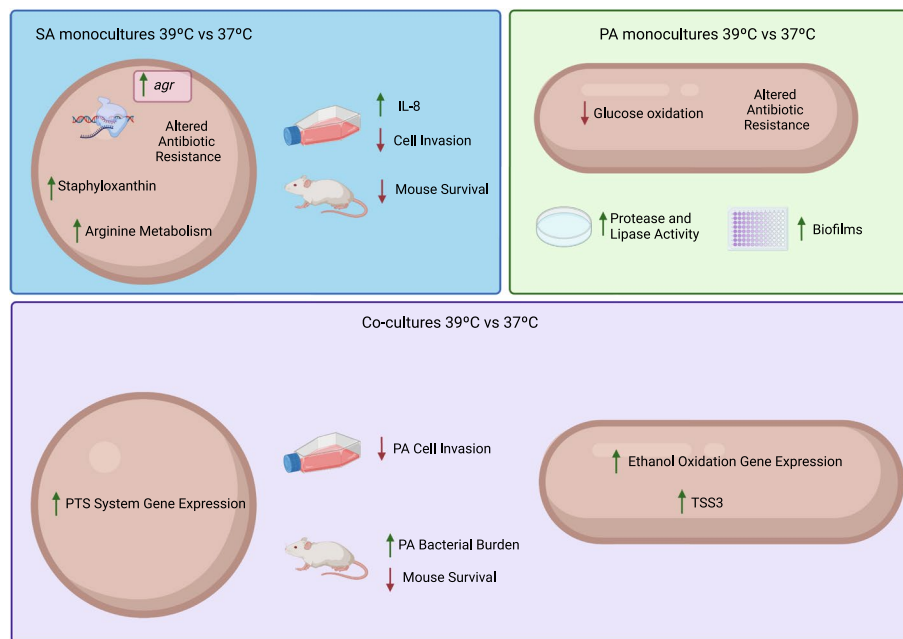


Fig. 8 Summary of the relevant effects of temperature on *S. aureus* USA300 and *P. aeruginosa* PAO1 monocultures and co-cultures

our findings at 37 °C align with these reports, at 39 °C, we observed pigment production even under microaerobic conditions. This heightened production may contribute to an increased virulence of PA at 39 °C.

The mechanism by which these bacterial species sense the increase in 2 °C and cause the observed phenotypes remains unknown. Thermoregulation through RNA thermometers has been described for SA but mostly for the environment-host transition and includes the *cspB*, *cspC*, and *cidA* genes [56, 57]. However, to our knowledge, the response to fever-like temperatures is still unknown. In PA, the sensing of temperature changes by RNA thermometers has also been reported for the virulence factors that are under the control of the quorum sensing regulator RhIR, including pyocyanin, elastase, and rhamnolipid production but, again, the differences were observed following a temperature shift from 30 to 37 °C [58].

Elevated body temperature additionally enhances the susceptibility of swiftly proliferating pathogens to eradication, synergistically interacting with other stressors like iron deprivation and the effect of antibiotics [47]. Therefore, the expression rearrangement and the increment in virulence factors could represent a bacterial response to cope with the stressful conditions during the acute phase response.

Conclusions

In conclusion, *S. aureus* (SA) and *P. aeruginosa* (PA) displayed different responses to fever-like temperatures. SA showed higher virulence gene expression, increased

hemolysis, and reduced biofilm formation and cell invasion as well as stimulated IL-8 production at 39 °C, suggesting enhanced pathogenicity. In contrast, PA demonstrates a more stable metabolism with fewer temperature-induced changes. Co-cultures exhibit complex interactions influencing metabolic pathways and lower PA invasion in A549 cells. Importantly, at 39 °C, co-cultures impact mouse survival, elevating PA burden in liver. Our findings suggest that temperature is not only an important cue that indicates the presence of the host but also indicates—when higher—the state of the host response for further bacterial adaptation and successful colonization.

Methods

Strains and culture conditions

The strains used throughout this work were *Staphylococcus aureus* USA300 (USA300_FPR3757) and *Pseudomonas aeruginosa* PAO1. Precultures were performed under aerobic conditions at 37 °C in Tryptic Soy Broth (TSB; Oxoid). Microaerobic cultures were grown in TSB supplemented with 0.5% KNO₃, in sealed bottles, using a 1:4 medium-to-flask volume ratio without agitation. SA and PA monocultures were inoculated at an OD_{600nm} of 0.05 and incubated at 37 °C for 2 h. After that, cultures were split in two and further incubated at 37 °C (control) or 39 °C (fever-like temperature) for 2 h. A similar protocol was used for co-culture experiments, where SA and PA were co-inoculated each at an OD_{600nm} of 0.05.

Plate competence assay

An overnight SA culture incubated at 37 °C was adjusted to an OD_{600nm} value of 1 and then seeded on a Tryptic soy agar (TSA) plate. A 5- μ l drop of a PA culture with an OD_{600nm} adjusted to 10 was placed in the center of the plate. After drying, the plates were incubated overnight at 37 or 39 °C.

RNA extraction and RNA library preparation

SA and PA monocultures or co-cultures were incubated at either 37 or 39 °C, following the experimental scheme shown in Additional File 1: Fig. S1. Frozen bacterial pellets were homogenized with milliQ water by using mortar and pestle devices in Eppendorf tubes. After cell disruption, total RNA was extracted with the Trizol method followed by extraction using a commercial kit (Total RNA extraction kit—RBC bioscience). Samples were treated with DNase I (Promega). To improve the quality of the readings, ribosomal RNA was depleted from the samples by Novogen services (CA, USA). Libraries were constructed by Novogen Services (CA, USA). Mass sequencing was performed using the Illumina Novaseq 6000 platform with a paired-end protocol (Novogen Services; CA, USA). For each condition, triplicate independent RNA extraction and libraries were used.

RNAseq data analysis

Reads were preprocessed using the Trimmomatic computer tool [59] by eliminating adapters and low-quality sequences. The reads quality was evaluated using the FastQC tool (www.bioinformatics.babraham.ac.uk/projects/fastqc/).

Reads alignment and assembly, transcript identification, and abundance quantification were carried out using the Rockhopper software for both monocultures and co-cultures [60]. The reference genomes were *P. aeruginosa* PAO1 (AE004091.2) and *S. aureus* (USA300_FPR3757). Reads were normalized per kilobase per million mapped reads. To verify concordance between the independent replicates for each condition, a Spearman correlation analysis of normalized counts was performed. Differential gene expression was considered only with $P < 0.05$ and $Q < 0.05$ and a Fold Change (FC) ≤ -1.5 and ≥ 1.5 . q -values are false discovery rate (FDR) adjusted p -values, using the Benjamini–Hochberg method. In the case of co-cultures, the RNA dataset was analyzed, and the reads aligned separately using the PA or SA reference genomes.

Genes were sorted into functional classes using the KEGG [61], MetaCyc [62], and String [63] tools. For

quantification and classification, tRNA transcripts were not considered.

RNAseq data is available in the European Molecular Biology Laboratory (<https://www.ebi.ac.uk/>) under accession number E-MTAB-12581 (<https://www.ebi.ac.uk/biostudies/arrayexpress/studies/E-MTAB-12581?key=6e13e32b-cae0-4154-9e08-1ccfa6fd46c8>).

Cultures and determination of organic acid production

To determine organic acid production, bacteria were grown in CDM [64] supplemented with 7.5 mM glucose as a carbon source. Cultures were centrifuged at 13,000 rpm for 5 min and supernatants were diluted 1:5 in water and filtered through 0.22- μ m syringe filters (MSI, USA). Samples were analyzed by high-performance liquid chromatography (HPLC) (LC-20AT Prominence; Shimadzu Corp., Japan) equipped with a UV detector (SPD-20AV; Shimadzu Corp.) using an Aminex HTX-87H column (Bio-Rad Laboratories, USA) at 50 °C. The mobile phase consisted of 5 mM H₂SO₄ with a flow rate of 0.6 ml/min. Detection was performed at 210 nm and analytical standards (Sigma-Aldrich Co., USA) were used for quantification by external calibration curves.

SA growth in arginine and proline-free medium

To assess arginine metabolism in SA, bacteria were grown in arginine- and proline-free modified CDM or in CDM supplemented with glucose 7.5 mM. SA was inoculated at an OD_{600nm} of 0.05 and cultures were incubated at 37 or 39 °C under microaerobic conditions, following the same scheme as described in Additional File 1: Fig. S1. After 4 h of incubation, the CFU ml⁻¹ in TSA was determined.

In vitro determination of virulence factors

The carotenoid pigment staphyloxanthin was quantified as previously described [65]. Briefly, cultures grown as described in Additional File 1: Fig. S1, the OD_{600nm} was adjusted to 1, and then 10 ml was centrifuged at 8000 rpm for 10 min. Cell pellets were washed with sterile PBS and resuspended in 1 ml of methanol. The tubes were incubated overnight in the dark with agitation at 37 °C. Then, the tubes were centrifuged to collect the supernatant containing the extracted pigments. Staphyloxanthin was quantified by measuring absorbance at 462 nm. For the evaluation of virulence factors, precultures were grown at 37 °C under aerobic conditions and the OD_{600nm} was adjusted to 1 for monocultures and for co-cultures in a 1:1 proportion for each bacterium, reaching an OD_{600nm} value of 1. With this bacterial suspension, a 5- μ l drop was placed in the corresponding plates and the plates were incubated at 37 or 39 °C for 24 h. DNase agar (Britania) was used following product instructions to analyze

extracellular DNase activity. Extracellular protease was determined using TSA plates supplemented with 5% skimmed milk. Rhamnolipid production was analyzed in sheep blood agar plates. Activity of extracellular lipases was analyzed using TSA plates supplemented with sterile egg-yolk suspension (5%). For all tests, the degradation halo or clear zone was measured in each case and the colony diameter was measured for normalization using the ImageJ software [66].

Antibiotic and H₂O₂ sensitivity assays

Antibiotic sensitivity was determined using the commercial panel Sensititre (Thermo Fisher) Gram positive for *S. aureus* USA300 and Gram negative for *P. aeruginosa* PAO1. The test was carried out strictly following the manufacturer's instructions, but the plates were incubated at 37 or 39 °C. The MIC was determined following the instructions. H₂O₂ sensitivity was evaluated in agar plates as previously [67]. Briefly, cultures grown as described in Figure S1 were seeded in a lawn, and a sterile Whatman no. 1 filter disc (6 mm) impregnated with 5 µM of 30% (v/v) H₂O₂ (Merck) was placed on the seeded plate. Plates were incubated only at 37 °C since the H₂O₂ effect is almost instant. Inhibition zones were measured using the ImageJ software.

Biofilm and motility assays

SA monocultures were seeded on Red Congo plates and then incubated overnight at 37 or 39 °C to detect exopolysaccharide production. Black-colored colonies were analyzed. Biofilm formation was analyzed in 96-multiwell polystyrene plates. Briefly, SA monocultures were inoculated at an initial OD_{600nm} of 0.025 in TSB supplemented with 0.5% KNO₃. Incubation was carried out at 37 or 39 °C for 24 h. Planktonic cells were collected and OD_{595nm} was measured. Biofilm was stained with crystal violet as described before [68], and the attached biomass was determined at 550 nm in a plate reader (DR—200Bs). For motility assays, the PA culture was adjusted to an OD_{600nm} of 1 (for co-cultures assay, the proportion was 1:1 for each bacterium) and a 5-µl drop was placed in a motility plate containing 8 g/l nutritive broth, 0.5% agar and supplemented with 0.5% glucose [69]. Plates were incubated overnight at 37 or 39 °C. The entire movement was measured using the ImageJ software.

Invasion assays on A549 cells

For invasion assays, A549 cells (a human adenocarcinoma epithelial cell line) were cultured at 37 °C under 5% CO₂ in Dulbecco's modified eagle medium (DMEM, Gibco) supplemented with 1% penicillin–streptomycin (Pen-Strep, Gibco) and 10% fetal bovine serum (FBS, Gibco). A549 cells were seeded in 24-well microtiter

plates at 2.5×10^5 cells per well and then incubated for 48 h (37 °C, 5% CO₂) in DMEM supplemented with 10% FBS and 1% Pen-Strep. Cells were washed twice with Dulbecco's Phosphate-Buffered Saline (DPBS – Gibco) to remove antibiotics and then 1 ml DMEM supplemented with 10% FBS. Cells were infected at a multiplicity of infection (MOI) of 30 for SA monocultures and of 20 for PA monocultures. For invasion experiments with co-cultures, after determining the CFU/ml to the OD₆₀₀ ratio of co-cultures, the OD_{600nm} was adjusted to 1. Then, 100 µl of this adjusted suspension was added to each well, which resulted in a MOI of 14 for SA and of 21 for PA. Bacteria and host cells were incubated for 1.5 h and then washed twice with DPBS. To kill extracellular bacteria, infected cells were incubated for 1.5 h in DMEM supplemented with 2.5 µg ml⁻¹ lysostaphin (Sigma) for SA or gentamicin 200 µg ml⁻¹ (Sigma) for PA infection or both for coinfections. Cells were washed again with DPBS and lysed with 0.1% Triton X-100, 0.5% trypsin, and 0.3 mg × ml⁻¹ DNase (Sigma) in DPBS. Serial dilutions of cell lysates were plated in TSA to quantify the internalized bacteria for monocultures. In the case of co-infected cells, the lysates were plated on TSA-NaCl to detect SA and in cetrimide agar to detect PA. Results are presented as a percentage of the internalized bacterial inoculum.

Cytokine measurements

For cytokine measurements, A549 cells were seeded in 96-well microtiter plates at a concentration of 5×10^4 cells per well for 24 h (37 °C, 5% CO₂) in DMEM (Gibco) supplemented with 10% FBS (Gibco) and 1% Pen-Strep (Gibco). After that, cells were washed with DPBS, and then 198 µl of fresh DMEM without antibiotics was added. Cells were stimulated by the addition of 2 µl of bacterial cultures (OD_{600nm} adjusted to 0.1). After 24 h of incubation (37 °C, 5% CO₂), plates were centrifuged, and the supernatants were used for cytokine determinations. Human cytokine secretion was measured using the Invitrogen enzyme-linked immunosorbent assay (ELISA) kits for IL-6 and IL-8 according to the manufacturer's instructions.

Bacterial inoculum for mouse lung infection experiments

SA and PA were cultured as previously described. Cells from monocultures and co-cultures were incubated at 37 or 39 °C and then harvested by centrifugation at 8000 rpm for 5 min, washed twice using sterile PBS and resuspended in PBS. The resuspended cells were then used to infect mice intranasally. For SA, mice were infected with 2×10^8 CFU per individual, whereas for PA infection, mice were infected with 1×10^7 CFU per individual. For co-cultures, the resuspension was adjusted to an OD₆₀₀ of 0.1 (corresponding to

a concentration of 1.4×10^7 CFU/ml for SA and 2.1×10^7 CFU ml⁻¹ for PA) and each mouse was infected with 200 μ L.

Mouse survival assay

Female DDY mice (6–8 weeks; 10 per group) were infected with SA monocultures at 37 and 39 °C, PA monocultures pre-incubated at 37 and 39 °C, or SA and PA co-cultures at 37 and 39 °C. Mice infected with sterile PBS were used as negative control. Mouse survival was monitored daily for 10 days. All experiments were carried out following the ethics guidelines and approved by the Institutional Ethics Committee of the University of Surabaya, Indonesia.

Bacterial burden assay

For the bacterial burden assay, six mice per group were infected using the same bacterial growth conditions as in the mouse survival assays. Mice were sacrificed 24 h after infection, and the lungs, kidney, and liver were aseptically recovered. These organs were then homogenized in sterile PBS containing 0.1% Tween 20. The bacterial load was determined by diluting the homogenized organ accordingly and plating on Mannitol Salt Agar (Merck) to count SA and Cetrinide Agar (Merck) to count PA. The CFU/ml were determined after 24 h incubation at 37 °C.

Bacterial count in the presence of human serum albumin (HSA)

Bacterial count was performed in TSB medium supplemented or not with HSA (3.5%) following the same scheme described above. Cultures were plated in TSA+NaCl and cetrinide agar plates for SA and PA determinations, respectively.

Statistical analysis

One- or two-way ANOVA with multiple comparisons or unpaired *t*-test was performed depending on the experiment, using GraphPad software (<https://www.graphpad.com/>). PCA was performed through the Singular Value Decomposition method on the normalized read counts. For multifactorial test applied to the entire RNAseq data set, two-way ANOVAs were carried out for each expression feature (genes) with factors: culture temperature (37 and 39 °C), type (mono and co-culture), and interaction. The *p*-values of the interaction terms were adjusted for multiple testing with the Benjamini–Hochberg method, the same used by Rockhopper, which will be subsequently called *q*-values for consistency with this tool. PCA and multiple ANOVAs were carried out in R programming language [70].

Abbreviations

SA	<i>Staphylococcus aureus</i> USA300
PA	<i>Pseudomonas aeruginosa</i> PAO1
Co	Co-cultures
Mono	Monocultures
Mono 39 vs 37	Comparison between monocultures incubated at 39°C and monocultures incubated at 37°C
Co 39 vs 37	Comparison between co-cultures incubated at 39°C and co-cultures incubated at 37°C
Co vs mono 37	Comparison between co-cultures incubated at 37°C and monocultures incubated at 37°C
Co vs mono 39	Comparison between co-cultures incubated at 39°C and monocultures incubated at 39°C
CFU/ml	Colony-forming units per milliliter
RNAseq	Total RNA sequencing
ANOVA	Analysis of variance
GOE	Gene Ontology Enrichment
TCA	Tricarboxylic acid
CDM	Complete defined medium
HPLC	High-performance liquid chromatography
PTS	Phosphotransferase system
FDR	False discovery rate
MIC	Minimal Inhibitory Concentration
TSS3	Type III secretion system
IL-6	Interleukin-6
IL-8	Interleukin-8
HSA	Human serum albumin

Supplementary Information

The online version contains supplementary material available at <https://doi.org/10.1186/s12915-024-01830-3>.

Additional file 1: Fig. S1. Pigment production and CFU counting under longer incubation periods. **Fig. S2.** Differentially expressed genes in *S. aureus* USA300. **Fig. S3.** Differentially expressed genes in *P. aeruginosa* PAO1. **Fig. S4.** Functional classification for *S. aureus* differentially expressed genes. **Fig. S5.** Functional classification for *P. aeruginosa* differentially expressed genes. **Fig. S6.** PCA analysis of differentially expressed genes. **Fig. S7.** Cytochrome expression for *S. aureus* and *P. aeruginosa*. **Fig. S8.** Interaction ANOVA of differentially expressed genes. **Fig. S9.** Representative images for virulence factor *in vitro* analysis.

Additional file 2: Table S1. Differentially expressed genes in *S. aureus*.

Additional file 3: Table S2. Differentially expressed genes in *P. aeruginosa*.

Additional file 4: Table S3. Gene Ontology Analysis for enriched pathways in *S. aureus* expression profile. **Table S4.** Gene Ontology Analysis for enriched pathways in *P. aeruginosa* PAO1 expression profile. **Table S5.** Metabolic features of *S. aureus*. **Table S6.** Relevant metabolic features in *P. aeruginosa*. **Table S7.** genes related to virulence that present in its expression interaction between temperature and culture condition in *S. aureus*. **Table S8.** Antibiotic sensitivity for *S. aureus*. **Table S9.** Antibiotic sensitivity for *P. aeruginosa*

Acknowledgements

We are thankful to Dr. Nancy I. Lopez for the proofreading of the manuscript and to Dr. Libera Lo Presti for editing.

Authors' contributions

ESV (under PMT and FG supervision) and PMT performed the conceptualization. ESV, MMR, MBG, SAR, DEE, and PMT performed most of the investigation. ABAZ and THM (under the supervision of AL) conducted mice studies. NB and JE (under the supervision of MSR) carried out the HSA protection experiments. FS, MMR, and DDP carried out data curation. NS performed the statistical analysis. PMT and ESV wrote the manuscript. FG, AL, and MMR reviewed and edited the manuscript. MMR, PMT, and ESV carried out the visualization. PMT performed mostly the project administration and funding acquisition. MSR, DDP, AL, and FG contributed with resources. All authors read and approved the final manuscript.

Funding

PMT discloses support for the research of this work from the ANPIDyl PICT 2018 N°2017 and by the Alexander von Humboldt Foundation (Equipment subsidy and Return Fellowship). FG discloses support for the research of this work from Cluster of Excellence EXC 2124—Controlling Microbes to Fight Infections—390838134. MSR discloses support for the research of this work from the National Institutes of Health (SC3GM125556). AL discloses support for the research of this work from Penelitan Keilmuan ITS 2022 (1022/PKS/ITS/2022). PMT, MMR, and DDP are career investigators from CONICET AL holds an Alexander von Humboldt. MBG, SAR, and FS have a doctoral fellowship from CONICET.

Availability of data and materials

RNAseq data is available in the European Molecular Biology Laboratory (<https://www.ebi.ac.uk/>) under accession number E-MTAB-12581 (<https://www.ebi.ac.uk/biostudies/arrayexpress/studies/E-MTAB-12581?key=6e13e32b-cae0-4154-9e08-1ccfa6fd46c8>) [71].

Declarations

Ethics approval and consent to participate

Mouse experiments using Female DDY mice (6–8 weeks) were carried out with the approval of the Institutional Ethics Committee, University of Surabaya, Indonesia, no. 108/KE/IX/2022, following all the ethics guidelines.

Consent for publication

Not applicable.

Competing interests

The authors declare that they have no competing interests.

Author details

¹Instituto De Química Biológica de La Facultad de Ciencias Exactas y Naturales-CONICET, Buenos Aires, Argentina. ²Department of Biology, Institut Teknologi Sepuluh Nopember, Surabaya, Indonesia. ³IFIBYNE (UBA-CONICET), FBMC, FCEyN-UBA, Buenos Aires, Argentina. ⁴Instituto del Calculo-UBA-CONICET, Buenos Aires, Argentina. ⁵Departamento de Química Biológica, FCEyN-UBA, Buenos Aires, Argentina. ⁶Department of Biological Science, College of Natural Sciences and Mathematics, California State University Fullerton, Fullerton, CA, USA. ⁷Department of Microbial Genetics, Interfaculty Institute of Microbiology and Infection Medicine Tübingen (IMIT), University of Tübingen, Tübingen, Germany. ⁸Present address Department of Biochemistry School of Medicine, Universidad Autónoma de Madrid and Instituto de Investigaciones Biomédicas Alberto Sols (Universidad Autónoma de Madrid-Consejo Superior de Investigaciones Científicas), Madrid, Spain.

Received: 31 July 2023 Accepted: 18 January 2024

Published online: 05 February 2024

References

- Wang M-G, Liu Z-Y, Liao X-P, Sun R-Y, Li R-B, Liu Y, et al. Retrospective data insight into the global distribution of carbapenemase-producing *Pseudomonas aeruginosa*. *Antibiotics*. 2021;10:548.
- Yebrá G, Harling-Lee JD, Lycett S, Aarestrup FM, Larsen G, Cavaco LM, et al. Multiclonal human origin and global expansion of an endemic bacterial pathogen of livestock. *Proc Natl Acad Sci U S A*. 2022;119:e2211217119.
- Cheung GYC, Bae JS, Otto M. Pathogenicity and virulence of *Staphylococcus aureus*. *Virulence*. 2021;12:547–69.
- Reynolds D, Kollef M. The epidemiology and pathogenesis and treatment of *Pseudomonas aeruginosa* infections: an update. *Drugs*. 2021;81:2117–31.
- Biswas L, Götz F. Molecular mechanisms of *Staphylococcus* and *Pseudomonas* interactions in cystic fibrosis. *Front Cell Infect Microbiol*. 2022;11:1383.
- Mashburn LM, Jett AM, Akins DR, Whiteley M. *Staphylococcus aureus* serves as an iron source for *Pseudomonas aeruginosa* during in vivo coculture. *J Bacteriol*. 2005;187:554–66.
- Voggu L, Schlag S, Biswas R, Rosenstein R, Rausch C, Götz F. Microevolution of cytochrome bd oxidase in *Staphylococci* and its implication in resistance to respiratory toxins released by *Pseudomonas*. *J Bacteriol*. 2006;188:8079.
- Biswas L, Biswas R, Schlag M, Bertram R, Götz F. Small-colony variant selection as a survival strategy for *Staphylococcus aureus* in the presence of *Pseudomonas aeruginosa*. *Appl Environ Microbiol*. 2009;75:6910–2.
- Szamosvári D, Böttcher T. An unsaturated quinolone N-oxide of *Pseudomonas aeruginosa* modulates growth and virulence of *Staphylococcus aureus*. *Angew Chem Int Ed*. 2017;56:7271–5.
- Camus L, Briaud P, Bastien S, Elsen S, Doléans-Jordheim A, Vandenesch F, et al. Trophic cooperation promotes bacterial survival of *Staphylococcus aureus* and *Pseudomonas aeruginosa*. *ISME J*. 2020;14:3093–105.
- Millette G, Langlois JP, Brouillette E, Frost EH, Cantin AM, Malouin F. Despite antagonism in vitro, *Pseudomonas aeruginosa* enhances *Staphylococcus aureus* colonization in a murine lung infection model. *Front Microbiol*. 2019;10:2880.
- Monteiro R, Magalhães AP, Pereira MO, Sousa AM. Long-term coexistence of *Pseudomonas aeruginosa* and *Staphylococcus aureus* using an in vitro cystic fibrosis model. 2021;16:879–93. <https://doi.org/10.2217/fmb-2021-0025>.
- Worlitzsch D, Tarran R, Ulrich M, Schwab U, Cekici A, Meyer KC, et al. Effects of reduced mucus oxygen concentration in airway *Pseudomonas* infections of cystic fibrosis patients. *J Clin Invest*. 2002;109:317–25.
- Pallett R, Leslie LJ, Lambert PA, Milic I, Devitt A, Marshall LJ. Anaerobiosis influences virulence properties of *Pseudomonas aeruginosa* cystic fibrosis isolates and the interaction with *Staphylococcus aureus*. *Scientific Reports*. 2019;9:1–18.
- Klinkert B, Narberhaus F. Microbial thermosensors. *Cell Mol Life Sci*. 2009;66:2661–76.
- Knapp BD, Huang KC. The effects of temperature on cellular physiology. *Annu Rev Biophys*. 2022;51:499–526.
- Yu KW, Xue P, Fu Y, Yang L. T6ss mediated stress responses for bacterial environmental survival and host adaptation. *Int J Mol Sci*. 2021;22:1–13.
- Loh E, Righetti F, Eichner H, Twittenhoff C, Narberhaus F. RNA thermometers in bacterial pathogens. *Microbiol Spectr*. 2018;6:55–73.
- Barbier M, Damron FH, Bielecki P, Suárez-Díez M, Puchałka J, Alberti S, et al. From the environment to the host: re-wiring of the transcriptome of *Pseudomonas aeruginosa* from 22°C to 37°C. *PLoS ONE*. 2014;9:e89941.
- Bastock RA, Marino EC, Wiemels RE, Holzschu DL, Keogh RA, Zapf RL, et al. *Staphylococcus aureus* responds to physiologically relevant temperature changes by altering its global transcript and protein profile. *mSphere*. 2021;6:10–128.
- Brewer SM, Twittenhoff C, Kortmann J, Brubaker SW, Honeycutt J, Massis LM, et al. A *Salmonella* Typhi RNA thermosensor regulates virulence factors and innate immune evasion in response to host temperature. *PLoS Pathog*. 2021;17:e1009345.
- Pienkoß S, Javadi S, Chaoprasid P, Holler M, Roßmanith J, Dersch P, et al. RNA thermometer-coordinated assembly of the *Yersinia* injectisome. *J Mol Biol*. 2022;434:167667.
- Tribelli PM, López NI. Insights into the temperature responses of *Pseudomonas* species in beneficial and pathogenic host interactions. *Appl Microbiol Biotechnol*. 2022;106:7699–709.
- Diard M, Hardt W-D. Evolution of bacterial virulence. *FEMS Microbiol Rev*. 2017;41:679–97.
- Ribet D, Cossart P. How bacterial pathogens colonize their hosts and invade deeper tissues. *Microbes Infect*. 2015;17:173–83.
- Abu Kwaik Y, Bumann D. Microbial quest for food in vivo: 'Nutritional virulence' as an emerging paradigm. *Cell Microbiol*. 2013;15:882–90.
- Lam O, Wheeler J, Tang CM. Thermal control of virulence factors in bacteria: a hot topic. *Virulence*. 2014;5:852.
- Balli S, Shumway KR, Sharan S. *Physiology*, Fever. 2022.
- Islam MA, Kundu S, Alam SS, Hossain T, Kamal MA, Hassan R. Prevalence and characteristics of fever in adult and paediatric patients with coronavirus disease 2019 (COVID-19): a systematic review and meta-analysis of 17515 patients. *PLoS ONE*. 2021;16:e0249788.
- González Plaza JJ, Hulak N, Zhumadilov Z, Akilzhanova A. Fever as an important resource for infectious diseases research. *Intractable Rare Dis Res*. 2016;5:97–102.

31. Saladin K. Major themes on anatomy and physiology. In: *Anatomy & Physiology: The Unity of Form and Function*. 6th ed. NY, USA: McGraw-Hill; 2011. p. 1–27.
32. Elhadad D, McClelland M, Rahav G, Gal-Mor O. Feverlike temperature is a virulence regulatory cue controlling the motility and host cell entry of typhoidal *Salmonella*. *J Infect Dis*. 2015;212:147–56.
33. Schlag S, Fuchs S, Nerz C, Gaupp R, Engelmann S, Liebeke M, et al. Characterization of the oxygen-responsive NreABC regulon of *Staphylococcus aureus*. *J Bacteriol*. 2008;190:7847–58.
34. Polack B, Dacheux D, Delic-Attree I, Toussaint B, Vignais PM. The *Pseudomonas aeruginosa* *fumC* and *sodA* genes belong to an iron-responsive operon. *Biochem Biophys Res Commun*. 1996;226:555–60.
35. Hempel N, Görisch H, Mern DS. Gene *ercA*, encoding a putative iron-containing alcohol dehydrogenase, is involved in regulation of ethanol utilization in *Pseudomonas aeruginosa*. *J Bacteriol*. 2013;195:3925–32.
36. Clauditz A, Resch A, Wieland KP, Peschel A, Götz F. Staphyloxanthin plays a role in the fitness of *Staphylococcus aureus* and its ability to cope with oxidative stress. *Infect Immun*. 2006;74:4950–3.
37. Pelz A, Wieland KP, Putzbach K, Hentschel P, Albert K, Götz F. Structure and biosynthesis of Staphyloxanthin from *Staphylococcus aureus*. *J Biol Chem*. 2005;280:32493–8.
38. Moormeier DE, Bayles KW. *Staphylococcus aureus* biofilm: a complex developmental organism. *Mol Microbiol*. 2017;104:365–76.
39. Quinn B, Rodman N, Jara E, Fernandez JS, Martinez J, Traglia GM, et al. Human serum albumin alters specific genes that can play a role in survival and persistence in *Acinetobacter baumannii*. *Sci Rep*. 2018;8:1–16.
40. Egesten A, Frick IM, Mörgelin M, Olin AI, Björck L. Binding of albumin promotes bacterial survival at the epithelial surface. *J Biol Chem*. 2011;286:2469–76.
41. Earn DJD, Andrews PW, Bolker BM. Population-level effects of suppressing fever. *Proceedings of the Royal Society B: Biological Sciences*. 2014;281:20132570.
42. Evans SS, Repasky EA, Fisher DT. Fever and the thermal regulation of immunity: the immune system feels the heat. *Nat Rev Immunol*. 2015;15:335–49.
43. Wurtzel O, Yoder-Himes DR, Han K, Dandekar AA, Edelheit S, Greenberg EP, et al. The single-nucleotide resolution transcriptome of *Pseudomonas aeruginosa* grown in body temperature. *PLoS Pathog*. 2012;8:e1002945.
44. Hamamoto H, Panthee S, Paudel A, Ohgi S, Suzuki Y, Makimura K, et al. Transcriptome change of *Staphylococcus aureus* in infected mouse liver. *Commun Biol*. 2022;5:721.
45. Reslane I, Halsey CR, Stastray A, Cabrera BJ, Ahn J, Shinde D, et al. Catabolic Ornithine Carbamoyltransferase activity facilitates growth of *Staphylococcus aureus* in defined medium lacking glucose and arginine. *mBio*. 2022;13:e00395–22.
46. Palela M, Giol ED, Amzuta A, Ologu OG, Stan RC. Fever temperatures impair hemolysis caused by strains of *Escherichia coli* and *Staphylococcus aureus*. *Heliyon*. 2022;8:e08958.
47. Wrotek S, Legrand EK, Dzialuk A, Alcock J. Let fever do its job The meaning of fever in the pandemic era. <https://doi.org/10.1093/emph/e0aa044>.
48. Sabat AJ, Pantano D, Akkerboom V, Bathoorn E, Friedrich AW. *Pseudomonas aeruginosa* and *Staphylococcus aureus* virulence factors as biomarkers of infection. *Biol Chem*. 2021;402:1565–73.
49. Laakso HA, Marolda CL, Pinter TB, Stillman MJ, Heinrichs DE. A heme-responsive regulator controls synthesis of Staphyloferrin B in *Staphylococcus aureus*. *J Biol Chem*. 2016;291:29.
50. Lin Y-C, Cornell WC, Jo J, Price-Whelan A, Dietrich LEP. The *Pseudomonas aeruginosa* complement of lactate dehydrogenases enables use of *d*- and *l*-lactate and metabolic cross-feeding. *mBio*. 2018;9:10–128.
51. Chekabab SM, Silverman RJ, Lafayette SL, Luo Y, Rousseau S, Nguyen D. *Staphylococcus aureus* inhibits IL-8 responses induced by *Pseudomonas aeruginosa* in airway epithelial cells. *PLoS ONE*. 2015;10:e0137753.
52. Alves PM, Al-Badi E, Withycombe C, Jones PM, Purdy KJ, Maddocks SE. Interaction between *Staphylococcus aureus* and *Pseudomonas aeruginosa* is beneficial for colonisation and pathogenicity in a mixed biofilm. *Pathog Dis*. 2018;76:fty003.
53. Oka T, Oka K, Kobayashi T, Sugimoto Y, Ichikawa A, Ushikubi F, et al. Characteristics of thermoregulatory and febrile responses in mice deficient in prostaglandin EP1 and EP3 receptors. *J Physiol*. 2003;551:945–54.
54. Shiraki C, Horikawa R, Oe Y, Fujimoto M, Okamoto K, Kurganov E, et al. Role of TRPM8 in switching between fever and hypothermia in adult mice during endotoxin-induced inflammation. *Brain Behav Immun Health*. 2021;16:100291.
55. Eskilsson A, Shionoya K, Engblom D, Blomqvist A. Fever during localized inflammation in mice is elicited by a humoral pathway and depends on brain endothelial interleukin-1 and interleukin-6 signaling and central EP₃ receptors. *J Neurosci*. 2021;41:5206–18.
56. Catalan-Moreno A, Cela M, Menendez-Gil P, Irurzun N, Caballero CJ, Caldelari I, et al. RNA thermoswitches modulate *Staphylococcus aureus* adaptation to ambient temperatures. *Nucleic Acids Res*. 2021;49:3409–26.
57. Hussein H, Fris ME, Salem AH, Wiemels RE, Bastock RA, Righetti F, et al. An unconventional RNA-based thermosensor within the 5' UTR of *Staphylococcus aureus* *cidA*. *PLoS One*. 2019;14:e0214521.
58. Grosso-Becerra MV, Croda-García G, Merino E, Servín-González L, Mojica-Espinosa R, Soberón-Chávez G. Regulation of *Pseudomonas aeruginosa* virulence factors by two novel RNA thermometers. *Proc Natl Acad Sci*. 2014;111:15562–7.
59. Bolger AM, Lohse M, Usadel B. Trimmomatic: a flexible trimmer for Illumina sequence data. *Bioinformatics*. 2014;30:2114–20.
60. Tjaden B. A computational system for identifying operons based on RNA-seq data. *Methods*. 2020;176:62–70.
61. Ogata H, Goto S, Sato K, Fujibuchi W, Bono H, Kanehisa M. KEGG: Kyoto Encyclopedia of Genes and Genomes. *Nucleic Acids Res*. 1999;27:29–34.
62. Caspi R, Billington R, Ferrer L, Foerster H, Fulcher CA, Keseler IM, et al. The MetaCyc database of metabolic pathways and enzymes and the BioCyc collection of pathway/genome databases. *Nucleic Acids Res*. 2016;44:D471–480.
63. Szklarczyk D, Gable AL, Lyon D, Junge A, Wyder S, Huerta-Cepas J, et al. STRING v11: protein–protein association networks with increased coverage, supporting functional discovery in genome-wide experimental datasets. *Nucleic Acids Res*. 2019;47:D607–13.
64. Vitko NP, Richardson AR. Laboratory maintenance of methicillin-resistant *Staphylococcus aureus* (MRSA). *Curr Protoc Microbiol*. 2013;28:9C–2.
65. Valliammai A, Selvaraj A, Muthuramalingam P, Priya A, Ramesh M, Pandian SK. Staphyloxanthin inhibitory potential of thymol impairs antioxidant fitness, enhances neutrophil mediated killing and alters membrane fluidity of methicillin resistant *Staphylococcus aureus*. *Biomed Pharmacother*. 2021;141:111933.
66. Schneider CA, Rasband WS, Eliceiri KW. NIH Image to ImageJ: 25 years of image analysis. *Nat Methods*. 2012;9:671–5.
67. Tribelli PM, Nickel PI, Oppezzo OJ, López NI. Anr, the anaerobic global regulator, modulates the redox state and oxidative stress resistance in *Pseudomonas extremaustralis*. *Microbiology*. 2013;159(Pt 2):259–68.
68. O'Toole GA, Kolter R. Flagellar and twitching motility are necessary for *Pseudomonas aeruginosa* biofilm development. *Mol Microbiol*. 1998;30:295–304.
69. O'May C, Tufenkji N. The swarming motility of *Pseudomonas aeruginosa* is blocked by cranberry proanthocyanidins and other tannin-containing materials. *Appl Environ Microbiol*. 2011;77:3061–7.
70. R Core Team. R: A language and environment for statistical computing. 2022.
71. Solar Venero E, Tribelli PM, Ricardi M. RNAseq of *Pseudomonas aeruginosa* PAO1 and *Staphylococcus aureus* USA300 in monocultures and co-cultivated at 37 and 39°C in microaerobiosis. Supplementary Datasets. BioStudies accession: E-MTAB-12581 <https://www.ebi.ac.uk/biostudies/arrayexpress/studies/E-MTAB-12581?key=6e13e32b-cae0-4154-9e08-1cfa6fd46c8>. 2023.

Publisher's Note

Springer Nature remains neutral with regard to jurisdictional claims in published maps and institutional affiliations.